Geothermal Energy

RESEARCH Open Access

The influence of thermal treatment on rock–bit interaction: a study of a combined thermo–mechanical drilling (CTMD) concept

Edoardo Rossi[1,2*], Martin O. Saar[1,3] and Philipp Rudolf von Rohr[2]

*Correspondence: rossie@ethz.ch
[1] ETH Zürich, Geothermal Energy and Geofluids Group, Sonneggstr. 5, 8092 Zurich, Switzerland
Full list of author information is available at the end of the article

Abstract

To improve the economics and viability of accessing deep georesources, we propose a combined thermo–mechanical drilling (CTMD) method, employing a heat source to facilitate the mechanical removal of rock, with the aim of increasing drilling performance and thereby reducing the overall costs, especially for deep wells in hard rocks. In this work, we employ a novel experiment setup to investigate the main parameters of interest during the interaction of a cutter with the rock material, and we test untreated and thermally treated sandstone and granite, to understand the underlying rock removal mechanism and the resulting drilling performance improvements achievable with the new approach. We find that the rock removal process can be divided into three main regimes: first, a wear-dominated regime, followed by a compression-based progression of the tool at large penetrations, and a final tool fall-back regime for increasing scratch distances. We calculate the compressive rock strengths from our tests to validate the above regime hypothesis, and they are in good agreement with literature data, explaining the strength reduction after treatment of the material by extensive induced thermal cracking of the rock. We evaluate the new method's drilling performance and confirm that thermal cracks in the rock can considerably enhance subsequent mechanical rock removal rates and related drilling performance by one order of magnitude in granite, while mainly reducing the wear rates of the cutting tools in sandstone.

Keywords: Thermal treatment, Granite, Deep geothermal, Rock–bit, Drilling performance, Rock removal, Thermally assisted drilling

Introduction

The construction of wells, for example to extract oil, gas or heat from underground reservoirs requires substantial financial investments, which are mainly related to the involved drilling operations (Tester et al. 2006; Akin and Karpuz 2008; Petty et al. 2009; Lukawski et al. 2014; Diaz et al. 2017). Additionally, the current trend of accessing deeper underground resources poses challenges for the overall project economics, as the costs increase exponentially with well depth (Fitzgerald 2013; Abdo and Haneef 2013; Hu et al. 2013). This is especially unfavourable for enhanced geothermal systems (EGSs) (Barbier 2002; Stefánsson 2002; Tester et al. 2006; Yost et al. 2015), which are

based on tapping underground heat to generate electricity by drilling 5–7 km deep into hard, crystalline rocks, such as granites (Mortensen 1978; Breede et al. 2013; Moore and Simmons 2013; Gan and Elsworth 2014; Amann et al. 2018; Gischig et al. 2019). Drilling of deep wells in hard rocks represents a major challenge for conventional rotary drilling methods. This challenge stems from rotary drilling methods removing rock mechanically. Such mechanical removal, particularly of hard (basement) rocks, results in poor drilling performances, in terms of high drill bit wear rates and low rates of rock penetration. This results in significant non-productive time, expensive tool replacements and poor process efficiencies, which drive up the overall project costs (Fay 1993; Wise et al. 2002; Diaz et al. 2017; Blankenship et al. 2005; Raymond et al. 2012). Therefore, recent drilling research has focused on implementing innovative solutions to improve the overall drilling process in hard rocks (Teodoriu 2011; Anders et al. 2015; Kant et al. 2017; Rudolf von Rohr et al. 2017; Kant et al. 2018; Reinsch et al. 2018; Beentjes et al. 2019).

In this work, in order to reduce the drilling efforts in hard rocks and foster accessing and utilizing deep georesources, we propose to combine conventional drilling with thermal assistance (Lauriello and Fritsch 1974; Rossi et al. 2018, 2020a). This method, based on a beneficial thermal weakening of the rock prior to mechanical rock removal, called Combined Thermo–Mechanical Drilling (CTMD) (Rossi et al. 2020a, b, c), is expected to facilitate the drilling process and provide a viable solution for drilling deep wells in hard formations. In a previous investigation, the material weakening after different thermal treatments was characterized together with the induced microstructural changes, showing good prospects for the investigated concept (Rossi et al. 2018). Nevertheless, to better investigate the feasibility of this drilling method, it is crucial to comprehend the related cutting characteristics, with a focus on the phenomena underlying the mechanical removal of thermally weakened rock, and assess the potential drilling performance improvements of this approach compared to conventional methods.

Extensive research has been carried out in the field of drilling to gain insights into the rock-cutting mechanisms and to improve the overall process performance, regarding penetration and bit lifetime (Zijsling 1984; Feenstra 1988; Che et al. 2012; Wang et al. 2017). The single-cutter approach (Zijsling 1987; Glowka 1989; Detournay and Defourny 1992; Wise et al. 2002; Hareland et al. 2009; Che et al. 2016; Munoz et al. 2016) is commonly used to answer fundamental questions regarding the rock-cutting process and, at the same time, provides a framework for tool development. Besides insights into the rock-cutting mechanisms, this approach also provides valuable inputs and validation means for drilling models (Franca 2011; Helmons et al. 2016; Zhou et al. 2017). West (1989) presented one interesting method, whose capabilities were later confirmed in the literature (Suana and Peters 1982; Al-Ameen and Waller 1994; Plinninger et al. 2003; Rostami et al. 2014; Abu Bakar et al. 2016). The convenience of this approach lies in the standardization of the abrasiveness property of rocks (ASTM 2010; Käsling and Thuro 2010; Alber et al. 2014), and enables also to gain insights into several parameters of interest concerning rock–bit interaction (Hamzaban et al. 2014).

In the present study, we aim at investigating, via laboratory testing, the feasibility of the CTMD technology and the fundamental mechanisms characterizing the rock-cutting process. In particular, we investigate the interaction between the rock and a cutting tool (i) to understand the phenomena behind the rock removal process, with a focus

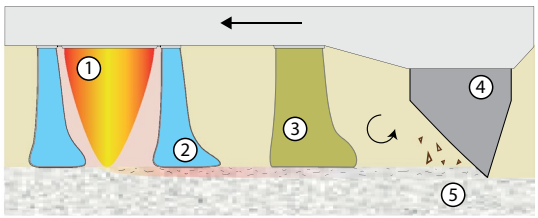

Fig. 1 Combined thermo–mechanical drilling. The combined thermo–mechanical drilling (CTMD) concept is based on thermally weakening the material prior to mechanical removal. The heat source (1), is protected by air shields (2) in the drilling fluid (3) environment at the drill bit. This allows the heat to reach the rock surface and thermally treat the material, which is then rapidly cooled down by the drilling fluid. Thereby, the weakened rock is finally removed by the cutter (4) which penetrates and drills the rock (5) with reduced effort. The drill bit moves from right to left in this illustration

on the conditions found during the proposed drilling concept, and (ii) we evaluate the drilling performance improvements, potentially achievable when a thermal source is implemented to assist the drilling process. To accomplish this, we present a novel testing apparatus, capable of capturing several rock–bit interaction parameters during the test. We investigate two rock materials, a sandstone and a granite, and we experimentally emulate the thermal assistance to drilling by a thermal treatment of the rock material prior to mechanical rock removal by a scratch test. In the remainder of this work, firstly, we introduce the concept of the CTMD method and, after this, we present the setup and experiment procedures. We present and further discuss the findings of this work, concerning tool penetration, wearing, as well as the mechanical tool response to rock-cutting, which provides evidence of the phenomena behind the rock–bit interaction. Finally, we demonstrate that the drilling performance can be greatly improved by assisting the process using a thermal source, especially in hard rocks, such as granite. We conclude this work by summarizing the findings on the rock removal characteristics of the proposed drilling technology and draw conclusions on its ease of implementation for deep, hard rock drilling prospects.

A combined thermo–mechanical drilling approach

In this work, we investigate the feasibility of a combined thermo–mechanical drilling (CTMD) method to improve the performance to drill deep wells in hard rocks. This method is based on employing a thermal source to facilitate the mechanical removal performed by conventional drilling cutters (Lauriello and Fritsch 1974; Rossi et al. 2018, 2020a). Conceptually, this approach exploits the fact that rocks, when exposed to heat, develop thermal stresses (Fredrich and Wong 1986), which are in turn responsible for thermal alterations of the internal structure and reduction of the mechanical properties of the rock (Yong and Wang 1980; Nasseri et al. 2009). In the context of a CTMD concept, several media can be used to provide the required heat to the surface (Maurer 1980), such as flame jets (Rossi et al. 2018) or laser jets (Jamali et al. 2017). These heat sources can be integrated into the conventional drilling system, providing great operational flexibility within rotary drilling methods. As conceptually shown in Fig. 1, the heat source, in this case a flame jet, is embedded next to drilling cutters and the bit face

rotates to remove the thermally weakened material. In order to increase the heat transfer efficiency of the flame jet, an air shielding configuration can be used, which constrains the heat to the rock surface and protects the flame jet from the circulation fluid used to transport the cuttings. In principle, the CTMD technology can be employed with various drilling fluid systems. The cutters finally remove the weakened rock with reduced effort, thereby increasing the overall drilling performance. In previous work (Rossi et al. 2018), we demonstrated the feasibility of using a thermal source to induce thermal weakening of rocks before rock removal.

In order to understand the rock removal characteristics and the resultant drilling performance when employing the proposed approach, we study, via laboratory testing, the interaction between a cutting tool and the rock. We experimentally emulate the thermal assistance to drilling by thermally treating the material prior to rock cutting for a sandstone and a granite.

Experiment materials and methods

In this work, we focus on two rock materials, namely, Rorschach sandstone and Grimsel granite, which are chosen as they represent two end-member conditions with respect to mechanical and mineralogical rock properties. The Rorschach sandstone is from Switzerland, and a thin section is shown in Fig. 2a. This rock consists of 35% quartz, 25% cements, 10% plagioclase, and 30% sedimentary lithics, with a fine-grain size distribution, ranging from 50 to 200 μm (Rossi et al. 2018). The Grimsel granite, also from Switzerland, is composed of 46% quartz, 31% feldspar, 20% plagioclase, 3% biotite and minor amounts of chlorite (Kant et al. 2017). A thin section of this rock is shown in Fig. 2b. The Grimsel granite exhibits a heterogeneous grain-size distribution, ranging from micrometers to a few millimeters. For the purpose of this study, rock block samples of size ($l \times w \times h$) 100×80×40 mm are saw-cut from larger blocks. During sample cutting, abundant cooling is provided to avoid any premature thermal damage of the rock. The samples' surfaces, where rock–bit interaction tests are conducted, exhibit initial surface roughness that is consistent with the saw-cutting procedure. No additional polishing of this surface is carried out.

In this study, the CTMD concept is experimentally emulated by thermally treating the rock samples prior to cutting. To ease the experiment procedure and accurately compare different conditions, a prior thermal treatment of the samples in an oven at high temperatures, followed by fast water-cooling is applied to represent, respectively, the heating by the thermal assistance to drilling and the subsequent cooling by the drilling fluid (water) environment prior to mechanical rock removal. From this, we compare the rock–bit interaction of the cutting tool for the two rock types under untreated and thermally treated conditions, representing the conventional and the proposed drilling approach, respectively. To treat the rock samples, we apply a constant heating rate in an oven (with a heating rate of 10 °C/s), reaching a maximum temperature of 800 °C. This treatment temperature is held for 30 minutes in order to avoid temperature gradients within the rock sample (Siddiqi and Evans 2015). With the aim of emulating continuous rock cooling during the drilling process, when the drilling fluid (water) is used to transport the rock cuttings, the rock samples are cooled down by flushing water right after the thermal

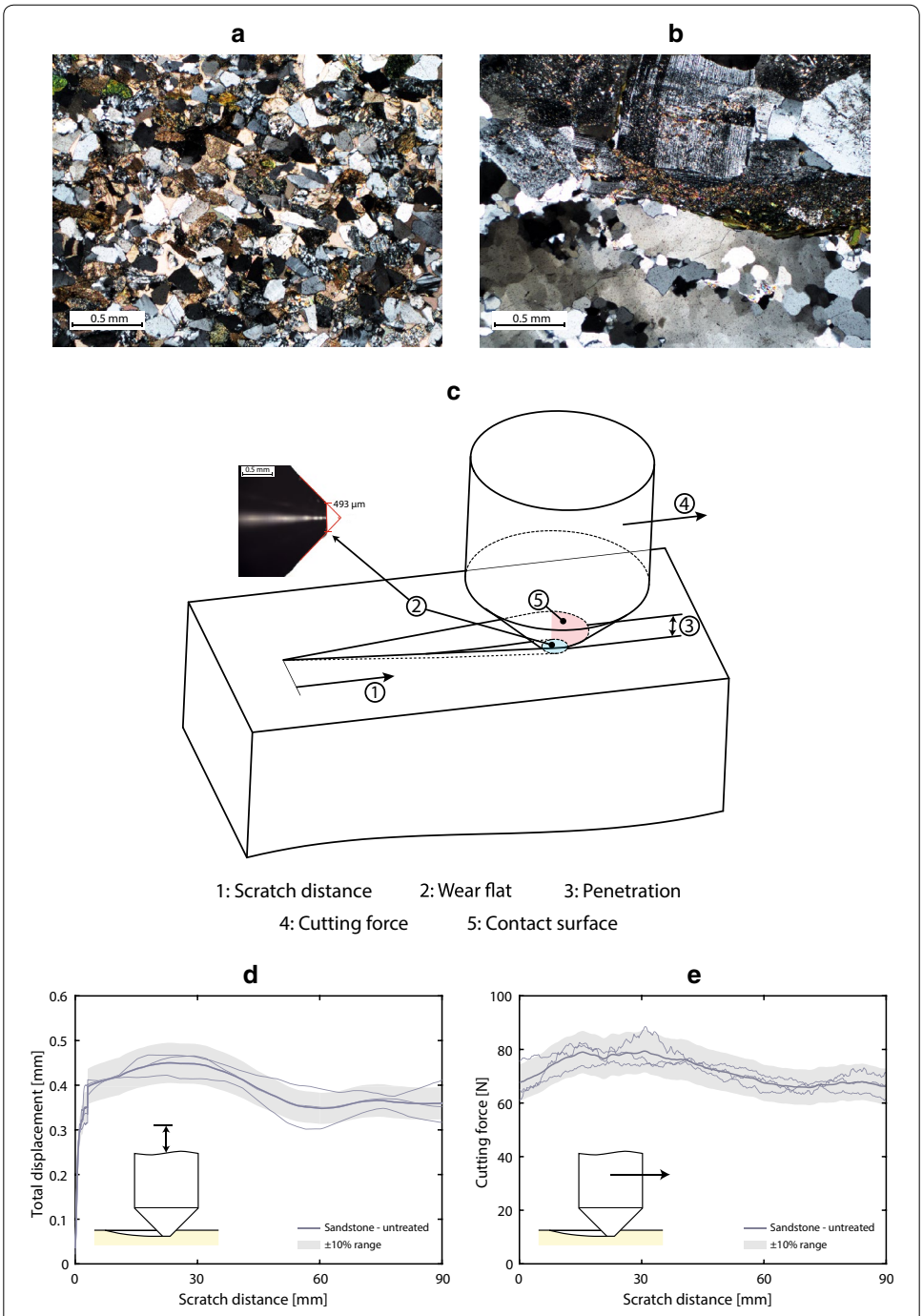

Fig. 2 Experiment methods and materials. Thin sections under cross-polarized light of the rock materials used in this work, i.e., Rorschach sandstone (**a**) and Grimsel granite (**b**). The experiment testing concept and the parameters measured to investigate rock–bit interaction are shown in **c**. During the experiments, the tool scratches the rock surface along a prescribed scratch distance (**c**.1), flattening the tool tip (**c**.2), which is optically imaged and investigated after the test. The tool penetration (**c**.3) and cutting forces (**c**.4) are monitored during the experiment. After the test, knowledge of wear flat and tool penetration enables determining the tool's contact surface (**c**.5). During the test, the total, vertical tool displacement is monitored (**d**) and afterwards processed, together with the wear flat at the tool tip to assess the actual penetration of the tool. During the test, the cutting forces exerted on the tool are measured as well (**e**). **d**, **e** The total displacement and cutting force signals obtained during several tests (thin lines), while the moving-averaged signal (thick line) is shown for comparison for the untreated sandstone material, together with the ±10% interval.

treatment in the oven. Thereafter, the samples are conserved under ambient laboratory conditions at room temperature, allowing the material to dry prior to testing.

Samples of Rorschach sandstone and Grimsel granite, under dry untreated and after-thermal-treatment conditions, are tested using the rock–bit interaction testing machine, shown in Fig. 2c. The setup was also preliminarily described in Rossi et al. (2018). The rock–bit interaction experiment consists of a scratch test of the sample, during which several removal characteristics parameters, together with tool wear, are quantified. Initially, the rock sample is placed in a clamping device and the horizontal alignment of the upper surface is checked. The cutting tool, used in this work, follows the guidelines in West (1989) and is a 10-mm-diameter cylindrical steel tool (material 115CrV3) with a 90°-conical sharp tip. This provides a unified measure of the wear flat at the tool tip, also referred to as Cerchar abrasivity index (CAI) (Cerchar 1973; ASTM 2010; Alber et al. 2014). From this, a constant vertical load of 70 N is prescribed to the scratching tool during the experiment (ASTM 2010). Furthermore, we modified the testing apparatus to permit accurate evaluations and correlations of removal parameters, such as scratching distance, tool penetration, cutting force and wear flat at the tool. The test is conducted along pre-defined scratch distances (see Fig. 2c.1) of up to 90 mm, as the tool advances into the rock, wearing out at the tip (wear flat in Fig. 2c.2). The rock sample is moved on a linear actuator, relative to the tool and along the scratch distance. After the test, the tool tip is inspected with a microscope at predefined scratch distances to measure the diameter of the wear flat (see exemplary picture in the top-left corner in Fig. 2c). Following the notation and standardization in (ASTM 2010), the wear flat value corresponds to 1/10 of the CAI value. Although we mainly focus on the wear flat in this work, the mentioned agreement with the CAI value can be useful for further comparisons of the presented results with literature work. The total vertical tool displacement into the rock material is continuously monitored during the scratching test by an inductive displacement sensor, placed on top of the scratching tool, as shown in Fig. 2d. The total vertical tool displacement measurement includes a contribution from the actual tool penetration onto the rock surface, and also the vertical displacement of the tool due to the wearing at the tool tip. Hence, the continuous monitoring of the total vertical tool displacement, as a function of scratch distance, and the imaging of the tool wear flat at predefined distances, enables the calculation of the actual tool penetration into the rock sample, as shown in Fig. 2c.3. During the scratch test, the cutting forces, required at the tool, resulting from the interaction between the tool and the rock material, along a direction parallel to the scratch direction, are continuously measured by the linear actuator (Fig. 2c.4). The force–scratch distance signals are shown, as an example, for the untreated sandstone in Fig. 2e. With the present experiment approach, another parameter, relevant to characterize the mechanical interaction between the rock sample and the scratching tool, is the contact surface (see red sector of the truncated cone in Fig. 2c.5), which is evaluated from the tool penetration and the wear flat at the tool tip.

In the next section, we correlate the main parameters, characterizing the rock–bit interaction tests for the two materials, sandstone and granite, under untreated and thermally treated conditions. After this, the measured parameters are summarized to evaluate removal performance parameters and provide conclusions regarding the

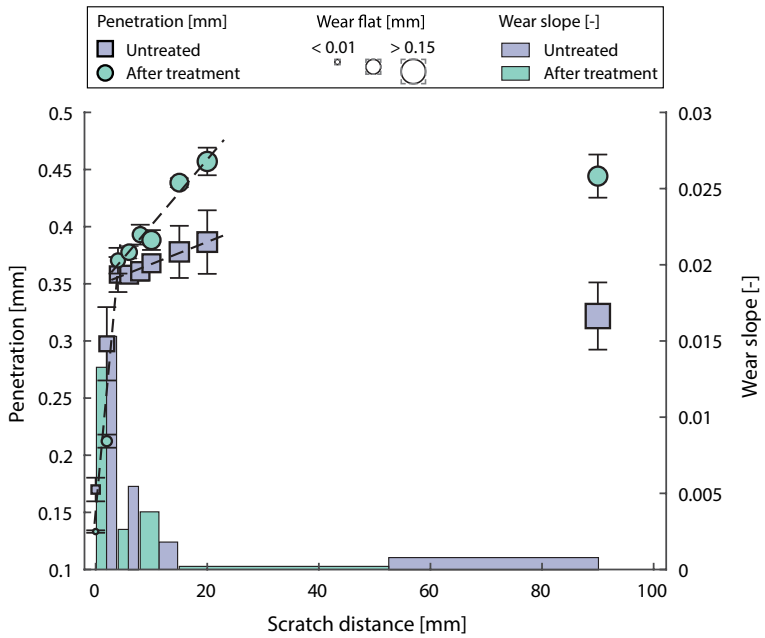

Fig. 3 Tool penetration and wear flat in sandstone. Tool penetration during testing of Rorschach sandstone is shown, with the scattered data and the left *y*-axis for untreated (violet squares) and after treatment (green circles). The symbol sizes represent the wear flattening of the cutting tool (see legend in the figure). The bi-linear regressions of the tool penetration values along the scratch distance are shown as dashed black lines. As a bar plot, we also include the wear flat increase per unit of scratch distance, here called wear slope, where the values are provided by the right *y*-axis. The bars indicate the wear slope for untreated (violet) and after-treatment (green) conditions, shown as contiguous columns for the scratch distance ranges 0–4 mm, 4–8 mm, 8–15 mm and 15–90 mm

enhancement of the cutting performance by thermally treating the rock before mechanical removal.

Results

Tool penetration

In this section, we present the experiment findings concerning the penetration of the cutting tool along the scratch distance. Treated material conditions (oven treatment followed by rapid water-cooling) are compared against the untreated case, firstly for Rorschach sandstone and subsequently for Grimsel granite. Thereafter, the standard deviations are calculated from three sets of experiments, conducted under the same conditions. The penetration of the tool in Rorschach sandstone is shown as a scatter plot in Fig. 3 for increasing scratch distances up to 90 mm.

In this figure, the wear flat, measured at the tool tip after the test, is indicated by the symbol sizes (see the legend in the figure). Furthermore, the right *y*-axis in Fig. 3 and the associated bar plot indicate the wear flat increase per unit of scratch distance, also called the wear slope, where values for the untreated and after-treatment cases are shown as contiguous columns within the scratch distance ranges. For both treatment conditions, i.e., untreated and after-treatment sandstone, we observe similar initial increases in tool penetration for scratch distances of 0–4 mm. This is followed by a second phase, characterized by a less-pronounced penetration of the tool into the rock. Especially, the

untreated material shows, for small scratch distances (< 4mm), a penetration increase per unit scratch distance of 0.05, decreasing to 0.0017 for scratch distances between 4 and 20mm (see dashed lines in Fig. 3, obtained from a bi-linear regression of the data). The treated-material case follows a similar trend as the untreated case, however, for the treated case and the scratch distance range 4–20 mm, we observe enhanced rock penetration depths with a tool penetration increase per unit of scratch distance of 0.0054. We note that the scratch distance, boundary for these two different tool penetration behaviors is with 4mm the same for the untreated and the treated cases, and is characterized by an abrupt penetration slope variation along the scratch distance. This slope change is found at a tool penetration of about 0.35 mm for both the untreated and after-treatment rock conditions. A differentiated trend between these two scratch distance ranges is also observed for the wear flat at the tool tip, shown by the symbol sizes, and the wear slope (wear flat increase with the scratch distance), indicated by the bars in Fig. 3. The wear of the tool appears to significantly increase mainly for scratch distances below 4mm. After this increase, the wear flat is almost constant for the scratch distance range of 4–20 mm, with wear flat values around 100 and 90 μm for the untreated and treated cases, respectively. As the scratch distance approaches 90 mm, the tool penetration reduces to slightly lower values. This is observed for both treatment conditions. We also notice that the mentioned decrease in rock penetration is followed by an almost unchanged wear flat at the tool tip. This is particularly visible for the untreated case. The delineated behavior of the tool penetration for large scratch distances can be appreciated in the exemplary plot in Fig. 2d, where the total vertical tool displacement signal is shown for the case of the untreated sandstone. As the wear flat at the tool tip can be considered constant for scratch distances above 20mm (see wear slopes in Fig. 3), the wear flat contribution to the calculation of the tool penetration is assumed to be negligible in this specific scratch distance range. Therefore, variations in total vertical tool displacements are directly related to variations in tool penetrations into the rock. Thus, we observe that, for large scratch distances and a consistently worn tool tip, the tool penetration into the rock tends to decrease and, furthermore, oscillate around smaller penetration values.

For the case of the Grimsel granite, the results are shown in Fig. 4. Here, as in Fig. 3, we present the tool penetration as scattered data points, and the corresponding wear flat values as the symbol sizes. The figure includes, as an inset figure, an enlarged plot for the scratch distance range 0–20 mm, where the wear slope along the scratch distance is also shown as a bar plot and the right y-axis. The standard deviation of the tool penetration data for Grimsel granite, shown in Fig. 4, is more significant, compared to the corresponding sandstone case, which is likely due to material heterogeneities (see thin sections in Fig. 2b) as well as the more brittle mechanical properties of Grimsel granite (Keusen et al. 1989; Rossi et al. 2018). Overall, we observe that, in the untreated granite case, the tool has a positive penetration value only for the first 8mm of scratch distance. Further, the tool penetration is always below 0.05mm. The wear flat at the tool tip occurs predominantly during the first 8 mm of scratch distance (see bars in the inset of Fig. 4), during which the tool penetrates the rock. In this scratch distance range, the wear flat at the tool tip steeply increases mainly during the first four millimeters of scratch distance and, after this, the reached high value of wear flat remains almost constant. A major increase of the wear flat is found during the first two millimeters of scratch distance, see

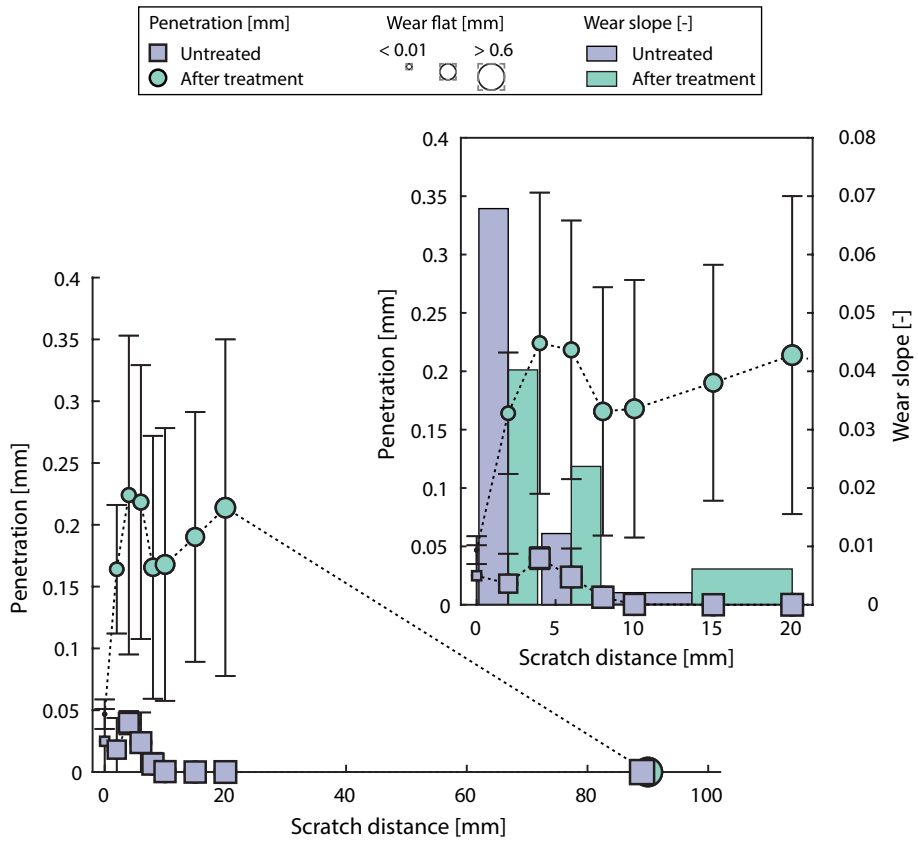

Fig. 4 Tool penetration and wear flat in granite. Tool penetration in Grimsel granite as a function of scratch distance is shown by the scatter plot and the left *y*-axis for untreated (violet squares) and after-treatment conditions (green circles). The symbol sizes represent the wear flat at the tool tip (see the legend in the figure). An enlargement of the figure for the 0–20 mm scratch distance range is shown in the inset figure. Here, the bar plot shows the wear flat increase per unit of scratch distance, i.e., the wear slope, where the values are given by the right *y*-axis. Contiguous bar pairs (violet for untreated and green for after-treatment conditions) are shown for the scratch distance ranges 0–4 mm, 4–8 mm and 8–20 mm. The overlapping data points at a scratch distance of 90 mm are shifted along the *x*-direction to visualize the wear flat (size of symbols)

the square sizes in the inset of Fig. 4. In the case of untreated granite, the tool is mainly sliding on the rock surface and no grooves are produced after the first 8mm. In contrast, the after-treatment case shows a substantially different behavior. As shown in Fig. 4, the tool penetration in thermally treated granite is a positive number for a wide range of scratch distances, with mean values fluctuating between 0.16 and 0.23 mm. These values are three to five times larger than those for untreated Grimsel granite. Furthermore, we observe that, after the tool penetration reaches a peak value of 0.23mm at a scratch distance of 4 mm (see inset in Fig. 4), the tool recedes and the wear flat slightly increases, before another increase in the tool penetration is found, with a peak at about 0.21mm at a scratch distance of 20mm. This second advancement phase of the tool is followed by its complete fall-back for a scratch distance of 90 mm, corresponding to a sliding regime of the cutting tool. A similar oscillating behavior of the tool penetration values along the scratch distance is also observed for the untreated material case. However, in the untreated case it is confined to a narrower scratch distance range of 0–8 mm (notice

the two consecutive peak penetration values reached within this range in the inset of Fig. 4). Concerning the wear flat for large scratch distances, it is interesting to consider the scratch distance range of 20–90 mm for the two treatment conditions. We observe that, for the case of thermally treated material, showing appreciable penetration values throughout the test, the wear flat significantly increases between scratch distances of 20 and 90 mm. In contrast, during the test with the untreated granite rock, showing limited tool penetration and only for the first 8mm of scratch distance, the wear flat at the tool tip is almost unchanged for the scratch distance range of 8-90 mm. Overall, we observe that the final wear flat at the maximum scratch distance for the treated material case is larger than that for the untreated granite case (scratch distance of 90mm in Fig. 4).

Contact surface

We report the contact surface area to characterize the interaction between the cutting tool and the rock, as the tool penetrates the material. From the wear flat at the tool tip and the tool penetration, it is possible to calculate the surface area of the tool that is in contact with the rock during the test. From these parameters, we determine the contact surface area as a function of scratch distance, for Rorschach sandstone and Grimsel granite (Fig. 5a and b, respectively). As shown above, the maximum penetration of the tool into the sandstone material is approximately twice that for the granite (compare Figs. 3 and 4). This is also reflected by the contact surface area results, which follow quadratic correlations, $k \cdot \delta^2$, where δ is the tool penetration and k is the multiplication constant (see the caption of Fig. 5 for the k-values for sandstone and granite). The results show that larger contact surface areas are reached for the thermally treated material (green circles in the figure). This is particularly visible for the granite, whose contact surface areas are always below 0.04 mm^2 under untreated conditions, whereas values of up to 0.35 mm^2 are reached after the granite has been thermally treated. In the granite case,

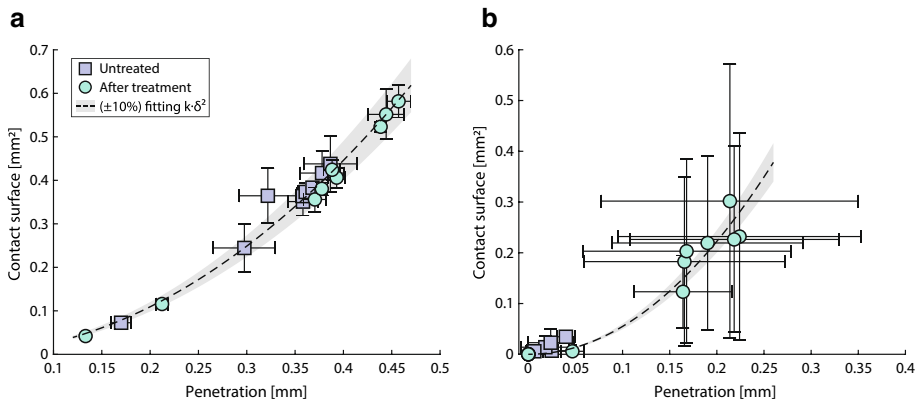

Fig. 5 Contact surface in sandstone and granite. The contact surface area variation (see also Fig. 2c.5) during the test is shown for Rorschach sandstone (**a**) and Grimsel granite (**b**) as a function of tool penetration into the rock. Untreated and post-treatment conditions are indicated by violet squares and green circles, respectively. The data are correlated by parabolic functions (dashed curves) of the type $S_c = k \cdot \delta^2$, where S_c is the contact surface, δ is the penetration depth, and the constants are empirically found here, and are given as $k = 2.86$ for Rorschach sandstone and $k = 5.75$ for Grimsel granite. The ±10% ranges are shown by the gray-shaded regions in **a** and **b**

the large data deviation, as also found for the tool penetration in Fig. 4, complicates further data analysis. Nevertheless, a clear trend can be observed for the mean values of several parameters.

Moreover, the contact surface area calculation shows that, as the multiplication constant, k, increases far above $k = \pi\sqrt{2}/2 \simeq 2.22$, the rock is very abrasive, as the cutting tool tip wears considerably for a given penetration of the tool into the rock (refer to the caption in Fig. 5 and compare the multiplication constant, k, for the two rock types). Therefore, the contact surface area and its increase for different tool penetration values can be used to (i) evaluate whether the rock abrasiveness will govern the test and (ii) estimate what type of rock removal mechanism the cutting tool will follow during rock penetration.

Hereafter, the contact surface areas are also extensively used to calculate the compressive stress state exerted by the rock on the tool during the test. The contact surface area also enables evaluating the volume of rock removed during the test, thereby providing an estimate of the removal performance parameters.

Cutting forces

In the following, the forces exerted on the cutting tool along a direction parallel to the tool's movement and measured by the linear actuator, are shown along the corresponding penetration of the tool in Rorschach sandstone, see Fig. 6a. We analyze the cutting forces, also considering the wear flat at the tool tip during the scratch test, represented

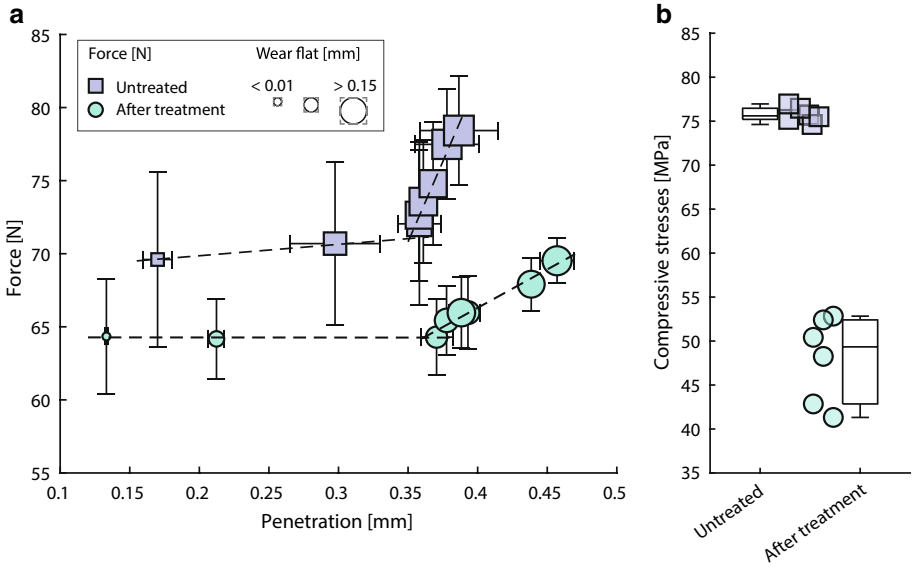

Fig. 6 Cutting forces in sandstone. The cutting forces exerted on the tool during the tests are shown in **a** as a scatter plot for Rorschach sandstone under untreated (violet squares) and after-treatment (green circles) conditions. Symbol sizes indicate the wear flat measured at the tool tip (see legend). Here, the curves obtained from bi-linear regressions of the data are shown as dashed lines. In **b**, the compressive stresses, exerted on the tool by the rock are calculated using the measured force values, the contact surface area under the stress state and a friction coefficient of 0.65 (Roshan et al. 2017). In **b**, the scattered data distributions, representing the strength of the rock, are summarized by boxes, where the central mark indicates the median value, the bottom and top edges of the box the 25th and 75th percentiles, respectively, and the error bars represent the standard deviation range

as symbol sizes in Fig. 6a (see legend). Comparisons between Figs. 3 and 6a enable us to correlate the cutting forces with the tool penetration along the scratch distance, and investigate the occurring cutting mechanisms. We observe in Fig. 6a that, as the tool penetrates the untreated sandstone, the cutting forces are almost constant for the initial tool penetration values, i.e., below about 0.35 mm. A similar behavior, however at smaller forces, is also found for the thermally treated material. In this first regime, we also notice that the tool's wear flat increases rapidly, analogously to the trend observed in Fig. 3 for small scratch distances. After this, as the tool penetration increases beyond 0.35 mm, the cutting forces increase promptly, following a linear trend, see dashed lines in Fig. 6a. The two material cases, untreated and thermally treated sandstone, show different slopes of the cutting forces versus penetrated depth in this second regime, as the force per unit penetration increases by 220 and 52 N/mm, respectively. Thus, we find an approximately four-times larger force increase as the tool penetrates the untreated Rorschach sandstone, compared to thermally treated conditions. In this second regime, i.e., when the tool penetration is $>$ 0.35 mm (also compare with Fig. 3), the wear flat does not appear to appreciably increase, despite the considerably intensified tool penetration (see symbol sizes in Fig. 6a). Furthermore, we calculate the compressive stresses exerted at the surface of the tool front during the creation of the groove for tool penetration values above 0.35 mm. We employ the contact surface area values, similar to the results shown in Fig. 5a, and the measured cutting force values. The resulting compressive stresses are presented in Fig. 6b. During the scratch test, we calculate compressive stresses of 75.7 ± 0.85 and 48.0 ± 4.90 MPa for untreated, and post-thermal-treatment sandstone conditions, respectively. As shown in this figure, the compressive stresses to remove the thermally treated material (green circles in Fig. 6b), are approximately 35% lower than those for the corresponding untreated sandstone conditions (violet squares).

Concerning Grimsel granite, we show in Fig. 7a the cutting forces measured as a function of tool penetration. The results for Grimsel granite yield larger standard deviations, compared to the sandstone results, as also observed for the tool penetration depth. This different behavior is mainly caused by the brittle and abrasive properties of Grimsel granite, as well as its heterogeneous microstructure, compared to Rorschach sandstone. In the case of untreated granite, the cutting tool slides on the rock surface for a considerable portion of the experiment, as also observed in Fig. 4. As shown in Fig. 7a, this sliding behavior corresponds to a constant cutting force of about 36 N. As the tool penetration into the untreated granite slightly increases, a sudden increase of the required force is measured, reaching values of up to around 50 N, see Fig. 7a. For the case of untreated granite, the limited penetration depth range, measured during the tests, does not allow a more systematic characterization of the relationship between cutting force and penetration depth. Regarding the thermally treated granite case, we observe that, for the only sliding point (scratch distance of 90 mm in Fig. 4), the cutting force value is around 40 N and, after this, the penetration steeply increases until values around 0.2 mm are reached. In contrast, the cutting forces reach values of $55-70$N, and the tool wears out rapidly, before receding towards lower penetration values. Although we do not measure penetration depths here in the range of $0.05-0.15$ mm, we suspect that the cutting forces likely follow a linearly increasing trend, as the tool penetrates the rock. Therefore, we observe that cutting forces show a distinct behavior as soon as positive tool penetration depths

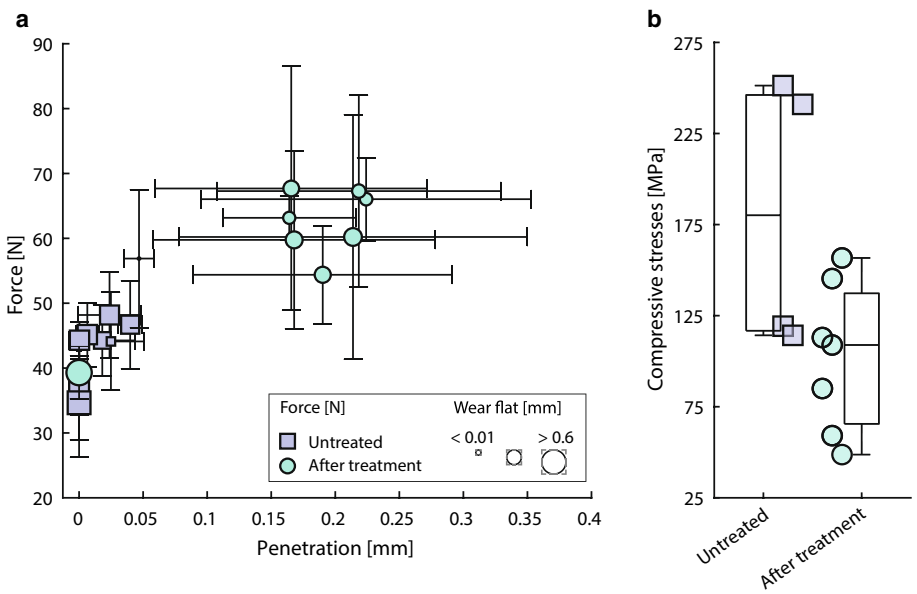

Fig. 7 Cutting forces in granite. The cutting forces exerted on the tool during the scratch experiment are shown in **a** as a scatter plot for Grimsel granite under untreated (violet squares) and after-treatment (green circles) conditions. Symbol sizes indicate the wear flat values measured at the tool tip (see legend). In **b**, the compressive stresses exerted on the rock during the test are calculated, using the measured forces and the projected surface area, calculated from the tool penetration depth and the wear flat values. In this plot, the scattered data distributions, representing the strength values, are summarized by boxes, where the central mark indicates the median value, the bottom and top edges of the box indicate the 25th and 75th percentiles, respectively, and the error bars represent the standard deviation range

are reached, and this is noticed both for untreated and after-treatment conditions (compare the cutting force trends for penetration depths larger than zero for the two cases in Fig. 7a). We calculate the compressive stresses, in Fig. 7b, from the measured forces, exerted when a scratch is created (positive penetrations). Despite smaller penetration depths in the untreated granite case and large deviations in the data, which introduce strong uncertainties when evaluating compressive stresses at the front surface of the cutting tool, we are able to compare the thermally treated to the untreated cases (Fig. 7b). We observe that, in the case of thermally treated granite, the compressive stresses are almost 45% smaller, compared to granite that has not been thermally treated.

Rock removal performance

We evaluate several cutting performance parameters from measured tool penetration depths, wear flat and cutting forces during the tests for the two rock types (granite and sandstone) and for untreated and after-thermal-treatment conditions. Rock removal and tool wear rates are calculated from the displaced rock volume and the worn volume of the cutting tool tip per unit of testing time, respectively (Rossi et al. 2018). These results are presented in Table 1. Concerning the rock removal rate, we observe that, after thermally treating Rorschach sandstone, this value increases by about 30%, compared to the untreated case. For Grimsel granite, a consistent increase in rock removal rate (by one order of magnitude) is achieved by thermally treating the material, as this value increases from 0.046 to 1.362 mm^3/min. Rorschach sandstone, a low-abrasiveness

Table 1 Summary of rock removal performance parameters. Rock removal performance parameters for Rorschach sandstone (left) and Grimsel granite (right), evaluated under untreated and after-treatment material conditions

	Sandstone		Granite	
	Untreated	After treatment	Untreated	After treatment
Removal rate [mm^3/min]	9.97	14.25	0.046	1.362
Wear rate [mm^3/min]	5.57×10^{-4}	1.43×10^{-4}	0.015	0.028
Performance ratio [–]	1.79×10^4	9.96×10^4	3.09	48.99
Specific energy [J/mm^3]	0.44	0.29	54.64	2.62

rock, shows reduced wear rates, for the case of thermally treated samples, by about 75% (Table 1). As shown above, in this rock, significant tool penetration depths are found during the entire test, both for untreated and thermally treated sandstone. In Grimsel granite, we observe improved removal rates after the rock has been thermally treated. However, this also corresponds to an increased wear rate of the cutting tool. Therefore, in the case of thermally treated granite, showing consistent tool penetration depths during the entire test and a limited sliding behavior of the tool, the wear rate is found to be higher, compared to the untreated rock case (Table 1). A more accurate measure of the drilling performance is given by the ratio of rock removal to tool wear rate. An increase of this parameter, also called the performance ratio in Table 1, is therefore an indication of improved overall performance of the rock removal process. As reported in Table 1, after thermally treating the granite rock, the performance ratio increases by one order of magnitude, compared to untreated material conditions. Additionally, we study the performance of the cutting process, also in terms of energy efficiency, by presenting results on the specific energy required to create the groove into the rock. The specific energy parameter represents the energy spent during the cutting process to remove a unit of rock volume from the sample surface (Maurer 1980). Here, the calculation of the specific energy does not take into account the thermal energy required to thermally treat the entire samples in the oven, as the actual heat treatment, by a flame jet, only heats a localized region in the sample. The results are shown in Table 1 for Rorschach sandstone and Grimsel granite. As displayed here, thermally treating the rock material before the scratch test yields considerable advantages from a cutting energy standpoint. This is evidenced in sandstone by a decrease in the required specific energy by more than 30%, when the rock is thermally treated, prior to cutting (Table 1). In Grimsel granite, we observe a significant improvement in rock removal efficiency, showing a reduction in the energy required, per volume of rock removed, by one order of magnitude, when thermal treatments are applied before cutting.

Discussion

In this work, we investigate the interaction between a cutting tool and two rock types, a granite and a sandstone, under untreated conditions and after thermal treatment. The presented experiment apparatus permits the continuous monitoring of the cutting tool tip during the creation of a groove and the evaluation of several parameters, such as the tool penetration depth, the wear flat, the tool's contact surface area, the required cutting

forces and the removed rock volume. In the sandstone material, we can distinguish three regimes concerning tool penetration, required cutting forces and tool wear flat. In the first regime, the cutting tool experiences a fast wearing and a consistent penetrated depth into the rock. After this, an abrupt variation of the measured tool penetration and wear flat is found at a penetration depth of about 0.35 mm. During this second regime, the wear rate is lower and the tool penetration increases linearly with scratch distance, following different slopes for the two treatment conditions. During the latter regime, the cutting forces also increase linearly with the penetration depth. The calculated compressive stresses for this regime are in agreement with the compressive strengths, measured elsewhere, employing similar testing methods (Richard et al. 2012; Rossi et al. 2018). The relative reduction of rock compressive strength after thermal treatment agrees with the findings by others (Liu and Xu 2015; Griffiths et al. 2017). Therefore, we propose that the cutting test can be divided into an initial wear-based phase, during which untreated and thermally treated rocks behave similarly, and a second phase, characterized by compressive-stress rock removal, which also permits an accurate determination of the rock's compressive strength. The bounding conditions between these two cutting regimes, regarding tool penetration depth and cutting forces, can be clearly appreciated for the sandstone rock under untreated and post-treatment conditions (see slope variations in Figs. 3 and 6). The granite material, on the other hand, due to its particularly abrasive nature (Plinninger et al. 2003; Hamzaban et al. 2014), wears out the cutting tool rapidly, so that the tool likely enters the compressive stage right away, as soon as a positive penetration is achieved (no sliding). This stage is evidenced in the granite material by intermittent peaking of the tool penetration depth along the scratch distance, followed by partial fall-back behaviors of the tool, presumably caused by a compressive stress balance at the tool tip whilst the tool wearing continues, when a constant normal load (70 N) is applied at the tool. Hence, we recognize a third stage, characterized by a receding phase of the tool penetration depth. During this third regime, in the case of sandstone, the penetrated depth stabilizes to lower penetration values. In contrast, in the case of granite, a complete fall-back of the cutting tool leads to a sliding behavior on the rock surface. Thus, focusing on the sandstone, we conclude that, for tool penetration depths below about 0.35 mm, the rock–bit interaction is a wear-based phenomenon and, as the penetration depth increases to values larger than 0.35 mm, the rock is removed satisfying a compressive-stress balance at the tool face. The present work agrees and further extends the conclusions presented in other publications, such as by Detournay and Defourny (1992), Richard et al. (1998, 2012), Huang et al. (2013) and He and Xu (2016), where the authors proposed that, for tool penetration depths smaller than about 1 mm, the removal mechanism follows a ductile failure mode, i.e., is governed by the compressive strength of the rock, which is based on the interplay between friction and cutting at small tool penetration depths (Detournay and Defourny 1992; Fairhurst and Lacabanne 1957; Zhou et al. 2017). In the present study, we demonstrate that there exists an initial wear-based regime in the tool penetration domain, whose presence and extent are likely a function of the rock's abrasiveness. This regime can also be described by the contact surface area function along the scratch distance, as shown in this work.

The compressive strength values, calculated using the measured cutting forces during the scratch tests, are in excellent agreement with the strength reductions observed by

Rossi et al. (2018). We notice that, after thermally treating the material, the rock strength decreases by 35% and 45% in Rorschach sandstone and Grimsel granite, respectively. This behavior of the material, after the oven-thermal treatment, can be explained by the heat-induced cracks in the rock microstructure (Kissell 1972; Fredrich and Wong 1986; Yong and Wang 1980; Nasseri et al. 2009; Tullis and Yund 1977; Wang et al. 1989; Meredith et al. 2001; Lin 2002; Freire-Lista et al. 2016; Griffiths et al. 2018; Rong et al. 2018; Han et al. 2019), caused by the differential thermal expansion of the quartz grains (Fredrich and Wong 1986; Glover et al. 1995) and by mineralogical changes in the rock (Ranjith et al. 2012; Xu et al. 2017), occurring at high temperatures. Furthermore, the fast cooling of the samples after the thermal treatment is likely responsible for enhanced cracking of the specimens (Kim et al. 2014; Shao et al. 2014; Browning et al. 2016; Wu et al. 2019) due to thermal shocking (Fellner and Supancic 2002; Kumari et al. 2017; Han et al. 2019), which, in turn, contributes to reducing the physical and mechanical integrity of the rock (Shao et al. 2014; Siratovich et al. 2015; Rathnaweera et al. 2018; Wu et al. 2019). Based on the performed experiments, we also compare drilling performance parameters, i.e., rock removal rates, wear rates and specific energy, for the case of untreated material, representing the conventional mechanical drilling case, and after thermally treating the rock, emulating the proposed combined thermo–mechanical drilling (CTMD) method. Different effects are observed after thermally treating the granite compared to the sandstone. In Rorschach sandstone, we find that the the wear rate is the main parameter affected by the thermal treatment of the rock. Here, the wear rate is consistently reduced (by almost 75%) by thermal rock treatment. In contrast, the rock removal is affected only to a small degree by the thermal treatment of the rock. An opposite behavior is found for the granite rock, where the cutting tool is capable of removing considerably more thermally treated rock (one order of magnitude larger), compared to the untreated case. Therefore, the material weakening, induced by the thermal cracks in the treated rock, is responsible for an enhanced penetration rate of the cutting tool in granite. In contrast, the enhanced penetration comes with an overall increased wear rate of the tip of the cutting tool, which is likely caused by the higher stresses on the cutting tool's tip when higher penetration rates are reached (Glowka 1989; Detournay and Defourny 1992; Gerbaud et al. 2006; Larsen-Basse 2014). Another important phenomenon to consider is the extensive sliding of the tool on the sample surface, observed during testing of the untreated granite case, which reduces the wear of the cutting tool. Overall, the performance ratio, considering both removal and wear rate, increases by one order of magnitude in the case of treated granite rock. As a further proof of the improved rock removal performance of the cutting tool in the thermally treated granite material, the specific energy is greatly reduced, witnessing the mechanical softening of the granite material from the drilling performance standpoint. The specific energy values, obtained from this fundamental analysis of required cutting forces, are found to agree with literature data (Maurer 1968). It is worth mentioning that our calculation of specific energy does not include the thermal energy required to heat the entire rock sample in an oven. In real drilling operations, the penetration rate is one of the main parameters influencing the economics of deep hard-rock drilling projects. In this context, improvements in penetration rate outweigh potential additional energy requirements.

Furthermore, the large deviation of the results, mainly observed during testing of Grimsel granite, and likely partially caused by rock heterogeneity and by the brittle nature of this rock, has introduced uncertainties when evaluating the data. All in all, by considering the calculated mean values of several parameters, it is nonetheless possible to extrapolate clear data trends and derive conclusions regarding the rock removal behavior and related rock removal performance, for both Rorschach sandstone and Grimsel granite.

Overall, we confirm that a thermal-cracking-based rock removal, which represents the basis of the investigated CTMD concept, may be extremely effective in enhancing rock drilling performance, especially in hard crystalline rocks, such as granite, by inducing intra- and inter-granular cracks in the rock structure (Lauriello and Fritsch 1974; Griffiths et al. 2017; Rossi et al. 2018; Nasseri et al. 2009). As a feasibility study of the proposed CTMD method towards its demonstration in the field, we perform, in this work, experiments in hard granite rocks, which are typically found in deep geothermal reservoirs and which are a major cause for the poor drilling performances of conventional drilling technologies (Pessier and Fear 1992). We present evidence that the proposed approach can greatly increase the drilling performance, highlighted by improved rock removal rates in a hard crystalline rock (granite) and a consistent reduction of wear rate in sandstone.

During the testing of the Grimsel granite, a sliding behavior of the cutting tool on the rock has been observed. This introduces difficulties in the evaluation of the tool penetration depth, the wear of the tool tip and the forces acting on the tool. Therefore, with the aim of improving CAI testing accuracy for hard rocks, such as granites, and limiting tool sliding, further research should focus on extending CAI procedures to also include, or change to, an increased normal load, applied to the tool (Al-Ameen and Waller 1994; Rostami et al. 2014). Such a load increase would ensure more consistent tool penetration depths during testing, likely yielding more robust test results, particularly regarding required cutting forces and induced tool wear.

Additionally, a more detailed characterization of the proposed CTMD approach for deep georesources requires specific investigations concerning the influence of deep in situ stress states on the presented rock removal mechanism and their effect on the overall process performance. Furthermore, in this work, we have experimentally emulated the thermal assistance during drilling by first heating the rock in an oven to high temperatures, followed by rapid water cooling of the rock. This procedure results in a spatially homogeneous and slow heating of the rock sample. Although the differences between slow and fast heating of rocks have been investigated in previous studies (Chen et al. 2017; Rossi et al. 2018; Shu et al. 2019), more research is required on the effectiveness of removal of flame-treated rocks by scratch tests. Such work should also investigate the effects of different heating rates on the overall drilling performance during CTMD.

The work presented here provides evidence for the fundamental feasibility of the proposed CTMD approach and its capability to improve the rock removal performance, especially in hard granitic rocks. The implementation of this new technology, particularly to drill deep boreholes in hard rocks, requires further studies and technical developments (Rossi et al. 2020a). Such research and development includes the process of

air-shielding the flame jets under high borehole fluid pressures. For example, the effects of different operational parameters on the effectiveness of air-shielding the flame jets (Rudolf von Rohr et al. 2017), including using different drilling fluids, varying drilling fluid columns (i.e., borehole fluid pressure) and, related, borehole cleaning requirements, need to be investigated, particularly for drilling deep wells. Additionally, the use of alternative solutions to provide the required heat downhole should be investigated. For instance, liquid reactants to achieve downhole combustion appear to be a safer and more feasible option than the combustion of gases downhole, especially when drilling deep.

Conclusions

This work investigates a novel combined thermo–mechanical drilling (CTMD) method, based on employing a heat source to thermally assist the mechanical rock removal, which is expected to reduce drilling efforts, by enhancing the drilling performance and provide a viable solution for drilling deep wells in hard formations. To accomplish this, we investigate the interaction between the cutting tool and two rock materials, a sandstone and a granite. We characterize the mechanisms behind the CTMD rock removal and their implications for improving drilling performance. We conclude that the tool penetration follows three distinct regimes: (i) an initial wear-dominated regime, (ii) a compression-based regime at larger penetrations, and (iii) a final fall-back regime of the tool after the maximum penetration depth has been reached, at constant vertical loads. Such a differentiation of cutting regimes, also comparing untreated and thermally treated rock, permits a deeper analysis of the weakening process, underlying the proposed combination of conventional drilling with thermal assistance. Further, the compressive strengths, measured during the second cutting regime, are in good agreement with previous work. Although some deviations of the results have been found, especially when testing hard granite rock, the mean values show clear trends that allow us to investigate the main drilling performance parameters. Thus, we evaluate the potential improvements of the proposed approach against conventional, i.e., mechanical drilling, by comparing rock removal and tool wear parameters during the testing of untreated and post-thermal-treatment rocks. We conclude that thermal treatment of rocks causes extensive thermally induced cracks in the rocks, which can significantly enhance the penetration performance (by up to one order of magnitude in granite) of the cutting tool, thereby reducing the mechanical effort required to remove rocks. Concerning the sandstone, the advantage of using the new CTMD method is mainly centered around a potential reduction in the drill bit wear rate. Therefore, the proposed approach, which provides thermal assistance to conventional drilling, is of interest particularly for accessing deep geological resources in hard, crystalline formations, with potential for significantly reducing the overall costs when drilling such rocks. Finally, we acknowledge that more research is required on improving the test procedures for hard rocks, such as granites, for example by increasing the load on the cutting tool, thereby reducing result uncertainties.

Acknowledgements
The authors are thankful to Daniel Birdsell for the helpful comments during the writing of this paper. We would also like to thank the editor and the anonymous reviewers for providing valuable feedback on an earlier version of the manuscript that improved this paper.

Authors' contributions
ER conducted the experiments, analyzed and interpreted the data, and drafted the manuscript. MS and PhRvR supervised the work and revised the manuscript. All authors read and approved the final manuscript

Funding
This work was supported by the Swiss Federal Office of Energy [grant SI/501'658-01]. We also thank the Werner Siemens Foundation (Werner Siemens-Stiftung) for its support of the Geothermal Energy and Geofluids (GEG.ethz.ch) group at ETH Zurich, Switzerland.

Availability of data and materials
Data presented in this work can be obtained upon request from the corresponding author Edoardo Rossi.

Competing interests
The authors declare that they have no competing interests.

Author details
[1] ETH Zürich, Geothermal Energy and Geofluids Group, Sonneggstr. 5, 8092 Zurich, Switzerland. [2] ETH Zürich, Institute of Process Engineering, Sonneggstr. 3, 8092 Zurich, Switzerland. [3] Department of Earth and Environmental Sciences, University of Minnesota, Minneapolis, MN, USA.

Received: 18 December 2019 Accepted: 11 May 2020
Published online: 27 May 2020

References

Abdo J, Haneef MD. Clay nanoparticles modified drilling fluids for drilling of deep hydrocarbon wells. Appl Clay Sci. 2013;86:76–82. https://doi.org/10.1016/j.clay.2013.10.017.
Abu Bakar MZ, Majeed Y, Rostami J. Effects of rock water content on CERCHAR Abrasivity Index. Wear. 2016;368–369:132–45. https://doi.org/10.1016/j.wear.2016.09.007.
Akin S, Karpuz C. Estimating drilling parameters for diamond bit drilling operations using artificial neural networks. Int J Geomech. 2008;8(1):68–73. https://doi.org/10.1061/(asce)1532-3641(2008)8:1(68).
Al-Ameen SI, Waller MD. The influence of rock strength and abrasive mineral content on the Cerchar Abrasive Index. Eng Geol. 1994;36:293–301. https://doi.org/10.1016/0013-7952(94)90010-8.
Alber M, Yarali O, Dahl F, Bruland A, Käsling H, Michalakopoulos TN, Cardu M, Hagan P, Aydın H, Özarslan A. ISRM Suggested method for determining the abrasivity of rock by the CERCHAR abrasivity test. Rock Mech Rock Eng. 2014;47:261–6. https://doi.org/10.1007/s00603-013-0518-0.
Amann F, Gischig V, Evans K, Doetsch J, Jalali R, Valley B, Krietsch H, Dutler N, Villiger L, Brixel B, Klepikova M, Kittila A, Madonna C, Wiemer S, Saar MO, Loew S, Driesner T, Maurer H, Giardini D. The seismo-hydromechanical behavior during deep geothermal reservoir stimulations: open questions tackled in a decameter-scale in situ stimulation experiment. Solid Earth. 2018;9:115–37. https://doi.org/10.5194/se-9-115-2018.
Anders E, Lehmann F, Voigt M. Electric impulse technology-long run drilling in hard rocks OMAE2015-41219. In: Proceedings of the ASME 34th International Conference on Ocean, Offshore and Arctic Engineering OMAE 2015, May 31-June 5, St. John's, Newfoundland, Canada, 2015.
ASTM D7625-10 – Standard test method for laboratory determination of abrasiveness of rock using the CERCHAR method. 2010:pp 6. https://doi.org/10.1520/D7625
Barbier E. Geothermal energy technology and current status: an overview. Renew Sust Energy Rev. 2002;6:3–65. https://doi.org/10.1016/S1364-0321(02)00002-3.
Beentjes I, Bender JT, Tester JW. Dissolution and thermal spallation of barre granite using pure water hydrothermal jets. Rock Mech Rock Eng. 2019;52(5):1339–52. https://doi.org/10.1007/s00603-018-1647-2.
Blankenship DA, Wise JL, Bauer SJ, Mansure AJ, Normann RA, Raymond DW, LaSala RJ. Research efforts to reduce the cost of well development for geothermal power generation ARMA/USRMS 05-884. In: Proceedings of the 40th US Symposium on Rock Mechanics (USRMS), Anchorage, Alaska, June 25-29, 2005.
Breede K, Dzebisashvili K, Liu X, Falcone G. A systematic review of enhanced (or engineered) geothermal systems: past, present and future. Geoth Energy. 2013;1(4):1–27. https://doi.org/10.1186/2195-9706-1-4.
Browning J, Meredith P, Gudmundsson A. Cooling-dominated cracking in thermally stressed volcanic rocks. Geophys Res Lett. 2016;43:8417–25. https://doi.org/10.1002/2016GL070532.
Cerchar A. Cerchar tests for the measurement of hardness and abrasivity of rocks. French Coal Ind. 1973;73–59:1–10.
Che D, Han P, Guo P, Ehmann K. Issues in polycrystalline diamond compact cutter-rock interaction from a metal machining point of view - Part II: Bit performance and rock cutting mechanics. J Manuf Sci Eng. 2012;134(6):064002. https://doi.org/10.1115/1.4007623 13 pp.
Che D, Zhu W-L, Ehmann K. Chipping and crushing mechanisms in orthogonal rock cutting. Int J Mech Sci. 2016;119:224–36. https://doi.org/10.1016/j.ijmecsci.2016.10.020.
Chen S, Yang C, Wang G. Evolution of thermal damage and permeability of Beishan granite. Appl Therm Eng. 2017;110:1533–42. https://doi.org/10.1016/j.applthermaleng.2016.09.075.
Detournay E, Defourny P. A phenomenological model for the drilling action of drill bits. Int J Rock Mech Min Sci. 1992;29(1):13–23. https://doi.org/10.1016/0148-9062(92)91041-3.
Diaz MB, Kim KY, Kang T-H, Shin H-S. Drilling data from an enhanced geothermal project and its pre-processing for ROP forecasting improvement. Geothermics. 2017;72:348–57. https://doi.org/10.1016/j.geothermics.2017.12.007.
Fairhurst C, Lacabanne W. Hard rock drilling techniques. Mine Quarry Eng. 1957;23:157–61.

Fay H. Practical evaluation of rock-bit wear during drilling SPE-21930-PA. SPE Drilling Compl. 1993;8(2):99–104. https://doi.org/10.2118/21930-PA.
Feenstra R. Status of polycrystalline-diamond-compact bits: Part I-Development SPE-17919-PA. J Pet Technol. 1988;40(6):675–84. https://doi.org/10.2118/17919-PA.
Fellner M, Supancic P. Thermal shock failure of brittle materials. Key Eng Mater. 2002;223:97–106. https://doi.org/10.4028/www.scientific.net/kem.223.97.
Fitzgerald T. Frackonomics: Some economics of hydraulic fracturing. Case W Res L Rev. 2013;63(4):1337–62. https://doi.org/10.3868/s050-004-015-0003-8.
Franca L. Drilling action of roller-cone bits: modeling and experimental validation. J Energy Resour Technol. 2011;132(4):043101, 9. https://doi.org/10.1115/1.4003168.
Fredrich JT, Wong TF. Micromechanics of thermally induced cracking in three crustal rocks. J Geophys Res. 1986;91(B12):743–64. https://doi.org/10.1029/JB091iB12p12743.
Freire-Lista D, Fort R, Varas-Muriel MJ. Thermal stress-induced microcracking in building granite. Eng Geol. 2016;206:83–93. https://doi.org/10.1016/j.enggeo.2016.03.005.
Gan Q, Elsworth D. Analysis of fluid injection-induced fault reactivation and seismic slip in geothermal reservoirs. J Geophys Res Solid Earth. 2014;119:3340–53. https://doi.org/10.1002/2013JB010679.
Gerbaud L, Menand S, Sellami H. PDC Bits: All comes from the cutter rock interaction. In: IADC/SPE Drilling Conference, 21–23 February, 2006, Miami, Florida. https://doi.org/10.2118/98988-MS.
Gischig V, Giardini D, Amann F, Hertrich M, Krietsch H, Loew S, Maurer H, Villiger L, Wiemer S, Bethmann F, Brixel B, Doetsch J, Doonechaly NG, Driesner T, Dutler N, Evans KF, Jalali M, Jordan D, Kittilä A, Ma X, Meier P, Nejati M, Obermann A, Plenkers K, Saar MO, Shakas A, Valley B. Hydraulic stimulation and fluid circulation experiments in underground laboratories: stepping up the scale towards engineered geothermal systems. Geomech Energy Environ. 2019;. https://doi.org/10.1016/j.gete.2019.100175.
Glover PWJ, Baud P, Darot M, Meredith PG, Boon SA, LeRavalec M, Zoussi S, Reuschlè T. α/β transition in quartz monitored using acoustic emissions. Geophys J Int. 1995;120:775–82. https://doi.org/10.1111/j.1365-246X.1995.tb01852.x.
Glowka DA. Use of single-cutter data in the analysis of PDC bit designs: Part 1-Development of a PDC cutting force model. J Pet Technol. 1989;41(8):797–849. https://doi.org/10.2118/15619-PA.
Griffiths L, Heap MJ, Baud P, Schmittbuhl J. Quantification of microcrack characteristics and implications for stiffness and strength of granite. Int J Rock Mech Min Sci. 2017;100:138–50. https://doi.org/10.1016/j.ijrmms.2017.10.013.
Griffiths L, Lengliné O, Heap MJ, Baud P, Schmittbuhl J. Thermal cracking in Westerly granite monitored using direct wave velocity, coda wave interferometry, and acoustic emissions. J Geophys Res Solid Earth. 2018;123:2246–61. https://doi.org/10.1002/2017JB015191.
Hamzaban M-T, Memarian H, Rostami J. Continuous monitoring of pin tip wear and penetration into rock surface using a new cerchar abrasivity testing device. Rock Mech Rock Eng. 2014;47(2):689–701. https://doi.org/10.1007/s00603-013-0397-4.
Han G, Jing H, Su H, Liu R, Yin Q, Wu J. Effects of thermal shock due to rapid cooling on the mechanical properties of sandstone. Environ Earth Sci. 2019;78(5):146–54. https://doi.org/10.1007/s12665-019-8151-1.
Hareland G, Yan W, Nygaard R, Wise JL. Cutting efficiency of a single PDC cutter on hard disk. JCPT. 2009;48(6):60–5. https://doi.org/10.2118/09-06-604.
He X, Xu C. Specific energy as an index to identify the critical failure mode transition depth in rock cutting. Rock Mech Rock Eng. 2016;49:1461–78. https://doi.org/10.1007/s00603-015-0819-6.
Helmons RLJ, Miedema SA, Alvarez Grima M, van Rhee C. Modeling fluid pressure effects when cutting saturated rock. Eng Geol. 2016;211:50–60. https://doi.org/10.1016/j.enggeo.2016.06.019.
Hu W, Bao J, Hu B. Trend and progress in global oil and gas exploration. Petrol Explor Dev. 2013;40(4):439–43. https://doi.org/10.1016/S1876-3804(13)60055-5.
Huang H, Lecampion B, Detournay E. Discrete element modeling of tool-rock interaction I: rock cutting. Int J Numer Anal Met. 2013;37:1913–29. https://doi.org/10.1002/nag.2113.
Jamali S, Wittig V, Bracke R. Mechanically assisted thermal type laserjet process for deep hard rock drilling. OIL GAS Euro Mag. 2017;43(4):192–6. https://doi.org/10.19225/171204.
Kant M, Rossi E, Madonna C, Höser D, Rudolf von Rohr P. A theory on thermal spalling of rocks with a focus on thermal spallation drilling. J Geophys Res Solid Earth. 2017;122(3):1805–15. https://doi.org/10.1002/2016JB013800.
Kant M, Rossi E, Duss J, Amann F, Saar MO, Rudolf von Rohr P. Demonstration of thermal borehole enlargement to facilitate controlled reservoir engineering for deep geothermal, oil or gas systems. Appl Energy. 2018;212:1501–9. https://doi.org/10.1016/j.apenergy.2018.01.009.
Käsling H, Thuro K. Determining rock abrasivity in the laboratory ISRM-EUROCK-2010-096. In: ISRM International Symposium - EUROCK2010, 15-18 June, Lausanne, Switzerland, 2010.
Keusen H, Ganguin J, Schuler P, Buletti M. Felslabor Grimsel Geologie - Technischer Bericht NTB 87–14. Nagra Geotest. 1989;166:169.
Kim K, Kemeny J, Nickerson M. Effect of rapid thermal cooling on mechanical rock properties. Rock Mech Rock Eng. 2014;47(6):2005–19. https://doi.org/10.1007/s00603-013-0523-3.
Kissell FN. Effect of temperature variation on internal friction in rocks. J Geophys Res. 1972;77(8):1420–3. https://doi.org/10.1029/JB077i008p01420.
Kumari WGP, Ranjith PG, Perera MSA, Chen BK, Abdulagatov IM. Temperature-dependent mechanical behaviour of Australian Strathbogie granite with different cooling treatments. Eng Geol. 2017;229:31–44. https://doi.org/10.1016/j.enggeo.2017.09.012.
Larsen-Basse J. Wear of hard-metals in rock drilling: a survey of the literature. Powder Metall. 2014;16(31):1–32. https://doi.org/10.1179/pom.1973.16.31.001.
Lauriello PJ, Fritsch CA. Design and economic constraints of thermal rock weakening techniques. Int J Rock Mech Min Sci Geomech Abstr. 1974;11(1):31–9. https://doi.org/10.1016/0148-9062(74)92203-7.

Lin W. Permanent strain of thermal expansion and thermally induced microcracking in Inada granite. J Geophys Res Solid Earth. 2002;107(B10):2215. https://doi.org/10.1029/2001JB000648.
Liu S, Xu J. An experimental study on the physico-mechanical properties of two post-high temperature rocks. Eng Geol. 2015;185:63–70. https://doi.org/10.1016/j.enggeo.2014.11.013.
Lukawski M, Anderson B, Augustine C, Capuano LE, Beckers KF, Livesay B, Tester JW. Cost analysis of oil, gas and geothermal well drilling. J Petrol Sci Eng. 2014;118:1–14. https://doi.org/10.1016/j.petrol.2014.03.012.
Maurer WC. Novel drilling techniques. New York: Pergamon Press; 1968. ISBN 0-87814-117-0.
Maurer WC. Advanced drilling techniques. Tulsa: The Petroleum Publishing Company; 1980.
Meredith PG, Knight KS, Boon SA, Wood I. The microscopic origin of thermal cracking in rocks: an investigation by simultaneous time-of-flight neutron diffraction and acoustic emission monitoring. Geophys Res Lett. 2001;28(10):2105–8. https://doi.org/10.1029/2000GL012470.
Moore J, Simmons S. More power from below. Science. 2013;340(6135):933–4. https://doi.org/10.1126/science.1235640.
Mortensen JJ. Hot dry rock: a new geothermal energy source. Energy. 1978;3(5):639–44. https://doi.org/10.1016/0360-5442(78)90079-8.
Munoz H, Taheri A, Chanda EK. Rock drilling performance evaluation by an energy dissipation based rock brittleness index. Rock Mech Rock Eng. 2016;49(8):3343–55. https://doi.org/10.1007/s00603-016-0986-0.
Nasseri MH, Schubnel A, Benson PM, Young RP. Common evolution of mechanical and transport properties in thermally cracked westerly granite at elevated hydrostatic pressure. Pure Appl Geophys. 2009;166:601–16. https://doi.org/10.1029/JB091iB12p12743.
Pessier RC, Fear MJ. Quantifying common drilling problems with mechanical specific energy and a bit-specific coefficient of sliding friction SPE-24584-MS. In: 67th Annual Technical Conference and Exhibition of the Society of Petroleum Engineers, Washington, DC, Oct 4–7, 1992. https://doi.org/10.2118/24584-MS.
Petty S, Lee Bour D, Livesay BJ, Baria R, Adair R. Synergies and opportunities between EGS development and oilfield operations and procedures SPE 121165. In: 2009 SPE Western Regional Meeting, San Jose, CA, March 24-26, 2009. https://doi.org/10.2118/121165-MS.
Plinninger R, Käsling H, Thuro K, Spaun K. Testing conditions and geomechanical properties influencing the CERCHAR abrasiveness index (CAI) value. Int J Rock Mech Min Sci. 2003;40(2):259–63. https://doi.org/10.1016/S1365-1609(02)00140-5.
Ranjith PG, Viete DR, Chen BJ, Perera MS. Transformation plasticity and the effect of temperature on the mechanical behavior of Hawkesbury sandstone at atmospheric pressure. Eng Geol. 2012;151:120–7. https://doi.org/10.1016/j.enggeo.2012.09.007.
Rathnaweera TD, Ranjith PG, Gu X, Perera M, Kumari W, Wanniarachchi W, Haque A, Li JC. Experimental investigation of thermomechanical behaviour of clay-rich sandstone at extreme temperatures followed by cooling treatments. Int J Rock Mech Min Sci. 2018;107:208–23. https://doi.org/10.1016/j.ijrmms.2018.04.048.
Raymond D, Knudsen S, Blankenship D, Bjornstad S, Barbour J, Schen A. PDC bits outperform conventional bit in geothermal drilling project. GRC Trans. 2012;36:307–16.
Reinsch T, Paap B, Hahn Simon, Wittig V, van der Berg S. Insights into the radial water jet drilling technology - application in a quarry. J Rock Mech Geotech Eng. 2018;10:236–48. https://doi.org/10.1016/j.jrmge.2018.02.001.
Richard T, Dagrain F, Poyol E, Detournay E. Rock strength determination from scratch tests. Eng Geol. 2012;147–148:91–100. https://doi.org/10.1016/j.enggeo.2012.07.011.
Richard T, Detournay E, Drescher A, Nicodeme P, Fourmaintraux D. The scratch test as a means to measure strength of sedimentary rocks SPE-47196-MS. In: SPE/ISRM Rock Mechanics in Petroleum Engineering, July 8-10, Trondheim, Norway, 1998. https://doi.org/10.2118/47196-MS.
Rong G, Peng J, Yao M, Jiang Q, Wong LNY. Effects of specimen size and thermal-damage on physical and mechanical behavior of a fine-grained marble. Eng Geol. 2018;232:46–55. https://doi.org/10.1016/j.enggeo.2017.11.011.
Roshan H, Masoumi H, Regenauer-Lieb K. Frictional behaviour of sandstone: a sample-size dependent triaxial investigation. J Struct Geol. 2017;94:154–65. https://doi.org/10.1016/j.jsg.2016.11.014.
Rossi E, Kant M, Madonna C, Saar MO, Rudolf von Rohr P. The effects of high heating rate and high temperature on the rock strength: feasibility study of a thermally assisted drilling method. Rock Mech Rock Eng. 2018;51(9):2957–64. https://doi.org/10.1007/s00603-018-1507-0.
Rossi E, Jamali S, Wittig V, Saar MO, Rudolf von Rohr P. A combined thermo-mechanical drilling technology for deep geothermal and hard rock reservoirs. Geothermics. 2020a;85:101771. https://doi.org/10.1016/j.geothermics.2019.101771.
Rossi E, Jamali S, Saar MO, Rudolf von Rohr P. Field test of a Combined Thermo-Mechanical Drilling technology. Mode I: Thermal spallation drilling. J Pet Sci Eng. 2020b;190:107005. https://doi.org/10.1016/j.petrol.2020.107005.
Rossi E, Jamali S, Schwarz D, Saar MO, Rudolf von Rohr P. Field test of a ccombined thermo-mechanical drilling technology. Mode II: Flame-assisted rotary drilling. J Pet Sci Eng. 2020c;190:106880. https://doi.org/10.1016/j.petrol.2019.106880.
Rossi E, Kant MA, Borkeloh O, Saar MO, Rudolf von Rohr P. Experiments on rock-bit interaction during a combined thermo-mechanical drilling method SGP-TR-213. In: Proceedings of the 43rd Workshop on Geothermal Reservoir Engineering, Stanford University, Stanford CA, Feb 12–14, 2018.
Rostami J, Ghasemi A, Gharahbagh EA, Dogruz C, Dahl F. Study of dominant factors affecting Cerchar abrasivity index. Rock Mech Rock Eng. 2014;47:1905–19. https://doi.org/10.1007/s00603-013-0487-3.
Shao S, Wasantha PLP, Ranjith PG, Chen BK. Effect of cooling rate on the mechanical behavior of heated Strathbogie granite with different grain sizes. Int J Rock Mech Min Sci. 2014;70:381–7. https://doi.org/10.1016/j.ijrmms.2014.04.003.
Shu R, Yin T, Li X. Effect of heating rate on the dynamic compressive properties of granite. Geofluids. 2019;8292065:1–12. https://doi.org/10.1155/2019/8292065.
Siddiqi G, Evans B. Permeability and thermal cracking at pressure in Sioux quartzite. J Geol Soc Lond. 2015;409(1):49–66. https://doi.org/10.1144/SP409.11.

Siratovich PA, Villeneuve MC, Cole JW, Kennedy BM. Saturated heating and quenching of three crustal rocks and implications for thermal stimulation of permeability in geothermal reservoirs. Int J Rock Mech Min Sci. 2015;80:265–80. https://doi.org/10.1016/j.ijrmms.2015.09.023.
Stefánsson V. Investment cost for geothermal power plants. Geothermics. 2002;31:263–72. https://doi.org/10.1016/S0375-6505(01)00018-9.
Suana M, Peters TJ. The cerchar abrasivity index and its relation to rock mineralogy and petrography. Rock Mech. 1982;15(1):1–8. https://doi.org/10.1007/BF01239473.
Teodoriu C. Use of downhole mud-driven hammer for geothermal applications SGP-TR-194. In: Proceedings of the 37th Workshop on Geothermal Reservoir Engineering, Stanford University, Stanford CA, Jan 30-Feb 01, 2011.
Tester JW, Anderson B, Batchelor A, Blackwell D, DiPippo R, Drake E, Garnish J, Livesay B, Moore MC, Nichols K. The future of geothermal energy. Technical Report: Idaho National Laboratory; 2006.
Tullis J, Yund R. Experimental deformation of dry Westerly granite. J Geophys Res. 1977;82(36):5705–18. https://doi.org/10.1029/JB082i036p05705.
Rudolf von Rohr P, Kant M, Rossi E. An apparatus for thermal spallation of a borehole. Patent EP3450675A1; 2017.
Wang H, Bonner B, Carlson R, Kowallis J, Heard H. Thermal stress vracking in granite. J Geophys Res Solid Earth. 1989;94(B2):1745–58. https://doi.org/10.1029/JB094iB02p01745.
Wang T, Xiao X, Zhu H, Zhao J, Li Y, Lu M. Experimental study on Longmaxi shale breaking mechanism with micro-PDC bit. Rock Mech Rock Eng. 2017;50:2795–804. https://doi.org/10.1007/s00603-017-1255-6.
West G. Rock abrasiveness testing for tunnelling. Int J Rock Mech Min Sci Geomech Abs. 1989;26(2):151–60. https://doi.org/10.1016/0148-9062(89)90003-X.
Wise JL, Raymond DW, Cooley CH, Bertagnolli K. Effects of design and processing parameters on performance of PDC drag cutters for hard-rock drilling. Trans Geoth Res Council. 2002;1:201–6.
Wu Q, Weng L, Zhao Y, Guo B, Luo T. On the tensile mechanical characteristics of fine-grained granite after heating/cooling treatments with different cooling rates. Eng Geol. 2019;253:94–110. https://doi.org/10.1016/j.enggeo.2019.03.014.
Xu F, Yang C, Guo Y, Wang T, Wang L, Zhang P. Effect of confining pressure on the mechanical properties of thermally treated sandstone. Curr Sci. 2017;112(6):1101–6.
Yong C, Wang C. Thermally induced acoustic emission in westerly granite. Geophys Res Lett. 1980;7(12):1089–92. https://doi.org/10.1029/GL007i012p01089.
Yost K, Valentin A, Einstein HH. Estimating cost and time of wellbore drilling for Engineered Geothermal Systems (EGS) - Considering uncertainties. Geothermics. 2015;53:85–99. https://doi.org/10.1016/j.geothermics.2014.04.005.
Zhou Y, Zhang W, Gamwo I, Lin J-S. Mechanical specific energy versus depth of cut in rock cutting and drilling. Int J Rock Mech Min Sci. 2017;100:287–97. https://doi.org/10.1016/j.ijrmms.2017.11.004.
Zijsling DH. Analysis of temperature distribution and performance of polycrystalline diamond compact bits under field drilling conditions SPE-13260-MS. In: SPE Annual Technical Conference and Exhibition, 16–19 September, Houston, Texas, 1984. https://doi.org/10.2118/13260-MS
Zijsling DH. Single cutter testing - A key for PDC bit development SPE-16529-MS. In: SPE Offshore Europe 87, 8-11 September, Aberdeen, Scotland, 1987. https://doi.org/10.2118/16529-MS.

Publisher's Note